



Gate-tuned superfluid density at the superconducting LaAlO₃/SrTiO₃ interface

Julie A. Bert,^{1,2} Katja C. Nowack,³ Beena Kalisky,^{3,4} Hilary Noad,³ John R. Kirtley,³ Chris Bell,¹ Hiroki K. Sato,¹ Masayuki Hosoda,¹ Yasayuki Hikita,¹ Harold Y. Hwang,^{1,3} and Kathryn A. Moler^{1,2,3,*}

¹Stanford Institute for Materials and Energy Sciences, SLAC National Accelerator Laboratory, 2575 Sand Hill Road, Menlo Park, California 94025, USA

²Department of Physics, Stanford University, Stanford, California 94305, USA

³Department of Applied Physics, Stanford University, Stanford, California 94305, USA

⁴Department of Physics, Nano-magnetism Research Center, Institute of Nanotechnology and Advanced Materials, Bar-Ilan University, Ramat-Gan 52900, Israel

(Received 17 May 2012; revised manuscript received 27 June 2012; published 7 August 2012)

The interface between the insulating oxides LaAlO₃ and SrTiO₃ exhibits a superconducting two-dimensional electron system that can be modulated by a gate voltage. While the conductivity has been probed extensively and gating of the superconducting critical temperature has been demonstrated, the question as to whether, and if so how, the gate tunes the superfluid density and superconducting order parameter needs to be answered. We present local magnetic susceptibility, related to the superfluid density, as a function of temperature, gate voltage, and location. We show that the temperature dependence of the superfluid density at different gate voltages collapses to a single curve that is characteristic of a full superconducting gap. Further, we show that the dipole moments observed in this system are not modulated by the gate voltage.

DOI: [10.1103/PhysRevB.86.060503](https://doi.org/10.1103/PhysRevB.86.060503)

PACS number(s): 74.78.Fk, 71.70.Ej, 74.25.N-, 75.20.-g

Electric field control of conducting channels has allowed great innovation in traditional semiconductor devices.¹ Now heterointerfaces in another class of materials, the complex oxides, have generated significant interest because of their gate tunable properties. Specifically, the conducting interface formed between the band insulators lanthanum aluminate and TiO₂ terminated 100 strontium titanate (LAO/STO)² exhibits many fascinating properties,³ suggesting that an electronic reconstruction triggered by the polar/nonpolar interface plays an important role in inducing the conductivity in the STO.⁴ At low temperatures this interface displays two-dimensional superconductivity.⁵ Additionally, the high dielectric constant of STO at low temperatures⁶ makes applying an electric field with a back gate especially effective to tune the properties of this superconducting state.

Caviglia *et al.* showed that, with increasing gate voltage V_g , the superconducting critical temperature T_c displayed a dome structure and concurrently the normal state resistance monotonically decreased.⁷ Later work showed that the electron mobility and carrier density both increased continuously with V_g , with the former dominating the V_g dependence of the conductivity.⁸ The evolution of a nonlinearity in the Hall resistivity as a function of V_g (Refs. 8 and 9) has been interpreted by Joshua *et al.* as evidence of electrons populating conduction bands with different mobilities,¹⁰ implying that the ratio of high and low mobility electrons may be tuned by gating.

Notably, the interface breaks spatial inversion symmetry, opening the possibility for spin orbit coupling to impact the electronic properties of the interface gas. Two groups reported tuning of the Rashba spin orbit coupling (RSOC) inferred from magnetoresistance^{11,12} and measurements of the in-plane critical fields.⁹ They found opposite dependencies for tuning the strength of the spin orbit coupling with V_g , making the impact of V_g on the spin orbit coupling unclear, possibly suggesting a peak in the spin orbit coupling.

Moreover, the discovery of magnetic patches that are coexistent with superconductivity^{13–15} and the presence of RSOC originating from the noncentrosymmetric nature of the interface have raised the possibility of an unconventional superconducting pairing mechanism or order parameter.^{16–18} However, previous measurements studying how gating affects the properties of the interface used electronic transport, which gives limited information about the superconducting state. In this Rapid Communication, we use local magnetic susceptibility to make direct measurements of the superfluid density in LAO/STO and address the question of how the superconducting state evolves with V_g .

Measurements were made on a sample with five unit cells (u.c.) of LAO grown at 800 °C and 1.3×10^{-5} mbar oxygen partial pressure on a TiO₂ terminated STO substrate. The growth was followed by a high pressure oxygen anneal, 600 °C in 0.4 bars. An elemental analysis on samples made with similar growth conditions in the same chamber shows that the magnetism is intrinsic and is not due to external contamination.¹⁹ The sample was silver epoxied to a piece of copper tape, which served as a back gate. V_g was applied between the copper tape and the interface, which was contacted by aluminum wire bonds. Magnetization and susceptibility measurements were made using a scanning superconducting quantum interference device (SQUID),²⁰ with a 3 μm diameter pickup loop and a concentric field coil for applying a local ac magnetic field. The pickup loop is sensitive to both the dc static flux and the ac flux resulting from diamagnetic screening currents canceling the field from the field coil. This setup enables simultaneous measurements of ferromagnetism and superconductivity in the sample.¹³

A superconductor will generate screening currents to screen an applied field. The currents extend into a bulk superconductor by the penetration depth λ . The temperature dependence of λ is a probe of the superconducting state. For a thin superconductor of thickness d , the screening distance is given

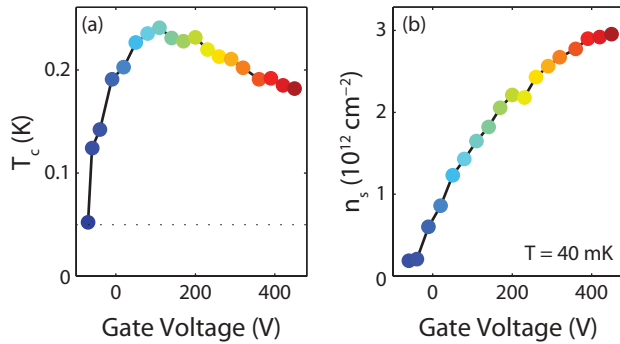


FIG. 1. (Color) (a) The critical temperature as a function of gate voltage forms a dome. The dashed line represents our lowest measurement temperature. (b) The superfluid density at our lowest temperature as a function of gate voltage. The superfluid density increases monotonically throughout the dome. The color scale represents gate voltage and is repeated in Fig. 2.

by the Pearl length $\Lambda = 2\lambda^2/d$.²¹ Using a model by Kogan,²² we extract Λ from measurements of the screening currents as a function of the distance between the sensor and the sample. Λ is related to the superfluid density, $n_s = 2m^*/\mu_0 e^2 \Lambda$, where e is the elementary charge, μ_0 the permeability of free space, and $m^* = 1.46m_e$ the effective electron mass measured by Ref. 23 from Shubnikov–de Haas on LAO/STO interfaces. We repeat these measurements at multiple temperatures and gate voltages to map out the superconducting state (Fig. 1). We define T_c as the temperature at which the diamagnetic screening drops below our noise level of $0.01\Phi_0/\Lambda$, corresponding to a minimum detectable n_s of $4\text{--}14 \times 10^{10} \text{ cm}^{-2}$. The statistical errors were smaller than the systematic errors, outlined in gray in Fig. 2(a), from imprecise knowledge of our measurement geometry.^{22,24} The systematic errors are fixed for a single cooldown and represent an overall scaling of n_s which would be the same for every measurement.

T_c vs V_g [Fig. 1(a)] has a maximum $T_c = 240$ mK. In the range of applied V_g superconductivity can only be eliminated on the underdoped side of the dome, and n_s grows monotonically with V_g , with $n_s = 3.0 \times 10^{12} \text{ cm}^{-2}$ at the largest V_g [Fig. 1(b)]. The carrier density and mobility were measured in a separate cooldown with no back gate. At 2 K the mobility was $1.02 \times 10^3 \text{ cm}^2/\text{V s}$ and the density was $2.05 \times 10^{13} \text{ cm}^{-2}$, ten times larger than the largest n_s we observed.

A small ratio of the superfluid density to the normal density is expected in the dirty limit, in which the elastic scattering time τ is much shorter than the superconducting gap Δ_0 ($\hbar/\tau \gg \Delta_0$). \hbar is the reduced Planck's constant. Above T_c the normal density of electrons n is given by the optical sum rule $n \propto \int_0^\infty \sigma_1(\omega) d\omega$, where σ_1 is the real part of the conductivity and ω the frequency. For a metal σ is sharply peaked near zero frequency, so scattering moves the spectral weight to higher frequencies. Below T_c , a gap opens at $\omega = 2\Delta_0/\hbar$ and the spectral weight within that gap collapses to a delta function at the origin whose amplitude is proportional to n_s .²⁵ Therefore, in the dirty limit, only a fraction of carriers enter the superconducting state, $n_s/n = 2\Delta_0/(\hbar/\tau)$. Using the gate tuned mobilities reported by Bell *et al.*, $100\text{--}1000 \text{ cm}^2/\text{V s}$,⁸

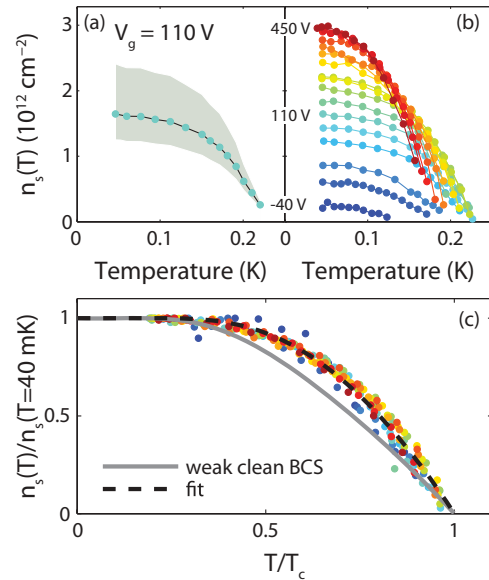


FIG. 2. (Color) (a) Superfluid density vs temperature for $V_g = 110$ V, the peak of the superconducting dome. The gray area shows a systematic error. (b) Superfluid density vs temperature for every gate voltage. The colors represent the same V_g from Fig. 1. (c) Normalized curves from (b). The gray line shows the temperature dependence of a weakly interacting clean BCS s -wave superconductor ($\Delta = 1.76$ and $a = 1$). The black dashed line is a fit to the data ($\Delta = 2.2$ and $a = 1.4$).

we expect the ratio n_s/n to be $0.01\text{--}0.1$, consistent with our measured n_s .

We now look at the temperature dependence of the superfluid density. Figure 2(b) plots n_s vs T for all V_g across the dome. Strikingly, when normalizing the curves they collapse [see Fig. 2(c)], showing that within our experimental errors there is no change in the superconducting gap structure with electrostatic doping. Furthermore, the collapse is reproducible over multiple positions, sweeps of V_g , and samples.²⁶

The temperature dependence of the superfluid density is a direct probe of the superconducting order parameter. It can be used to distinguish BCS superconductors from unconventional superconductivity. We fit the normalized curves to a phenomenological BCS model with two parameters Δ and a .²⁸ Δ scales the superconducting gap $\Delta_0 = \Delta k_B T_c$. a is a shape parameter that determines how rapidly the gap opens below T_c , $n_s \propto 1 - (T/T_c)^{2a}$,^{27–29} $\Delta = 1.76$ and $a = 1$ for a clean s -wave BCS superconductor with weak coupling,²⁸ plotted as the gray line in Fig. 2(c). The fit to our data gives $\Delta = 2.2$ and $a = 1.4$. This is consistent with a BCS description with increased coupling or disorder. Both will theoretically increase the gap and the a parameter,³⁰ shifting the curve up and to the right.

The flattening at low temperature indicates a fully gapped behavior with a gap that is larger than BCS weak-coupling s wave. Our lowest measurement temperature is $1/6$ of T_c^{max} , and n_s remains flat (within 3%) up to 35% of T_c . A full gap indicates the absence of low energy quasiparticle excitations, ruling out order parameters with nodes in the Fermi surface. Furthermore, the steep rise of n_s near T_c and the absence of a kink in the functional form rule out most weak-coupling

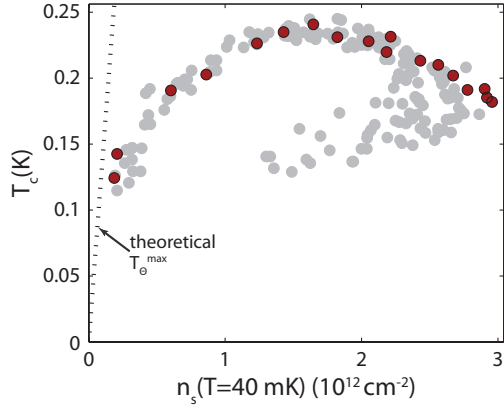


FIG. 3. (Color) Critical temperature vs the superfluid density at lowest temperature ($T \sim 40$ mK). The red points are the data from Fig. 1 and the gray dots represent additional data sets. The dotted line is the theoretical phase fluctuation temperature from Ref. 32, which may be limiting the critical temperature on the underdoped side of the dome. The bimodal distribution on the overdoped side is due to inhomogeneity that locally suppresses n_s in different regions of the sample while the T_c remains the same. See also Fig. 4.

two-band models,³¹ because a second smaller gap will slow the onset of superconductivity near T_c . Two gaps of similar size, both larger than the BCS gap or a dominant single large gap with a second smaller amplitude gap, could reproduce the data.

The low n_s in the underdoped region may result in the suppression of T_c by thermal phase fluctuations. Such fluctuations would result in a linear temperature dependence of n_s in the underdoped region. Following Ref. 32, we calculate a phase ordering temperature, $T_\theta^{\max} = A\hbar^2 n_s(0)/4m^*$, where $A = 0.9$ in two-dimensional (2D) systems. Figure 3 shows T_c vs n_s (40 mK), and additionally T_θ^{\max} is plotted as a linear function of n_s : The line does not suggest a fit to our data. We have insufficient data at the lowest superfluid densities to make any statement about the functional form of $T_c(n_s)$ in the region where phase fluctuations may be limiting T_c . Nevertheless, the proximity of the phase ordering line to the underdoped data suggests that phase fluctuations may drive the abrupt decrease of T_c .

Given the 2D nature of the superconducting system we expect a Berezinsky-Kosterlitz-Thouless (BKT) transition, where unbinding of vortex-antivortex pairs suppresses superconductivity and results in a discontinuous jump in n_s near T_c . The jump should occur at a finite superfluid density $n_s = 2m^*T_c/\pi\hbar^2$.³³ For the maximum $T_c = 240$ mK a BKT transition should occur at $5 \times 10^{10} \text{ cm}^{-2}$, which is too close to our measurement threshold to establish a BKT jump in our n_s vs T curves.

Are our observations consistent with a simple s -wave order parameter from doped STO³⁴ or a two-gap mixed state induced by symmetry breaking at the interface? Rashba spin orbit coupling (RSOC), induced by the structural inversion asymmetry, is expected to lift the spin degeneracy and split the energy bands.³⁵ Additionally, RSOC breaks parity and consequently mixes singlet and triplet states, resulting in an s -wave component Δ_s mixed with a triplet induced d

vector, $\mathbf{d}(\mathbf{k}) = \hat{x}k_y - \hat{y}k_x$.^{18,36} Mixing results in two gaps, $\Delta = \Delta_s \pm |d_k|$, whose magnitudes depend on the weights of the singlet and triplet components. Varying the relative weights changes the density of states, but always results in two fully gapped Fermi surfaces except for the special case where the s -wave singlet and triplet gaps are the same and accidental line nodes form on one band.¹⁸

Other reports^{9,11} have demonstrated significant tuning of the strength of RSOC with V_g . An open question, of particular importance to testing this two-gap picture, is how do the weight of the two components change with V_g . Our results, showing a consistent functional form for n_s vs T across all V_g , show that the superconducting gap structure does not change with V_g and consequently the relative gap weights do not

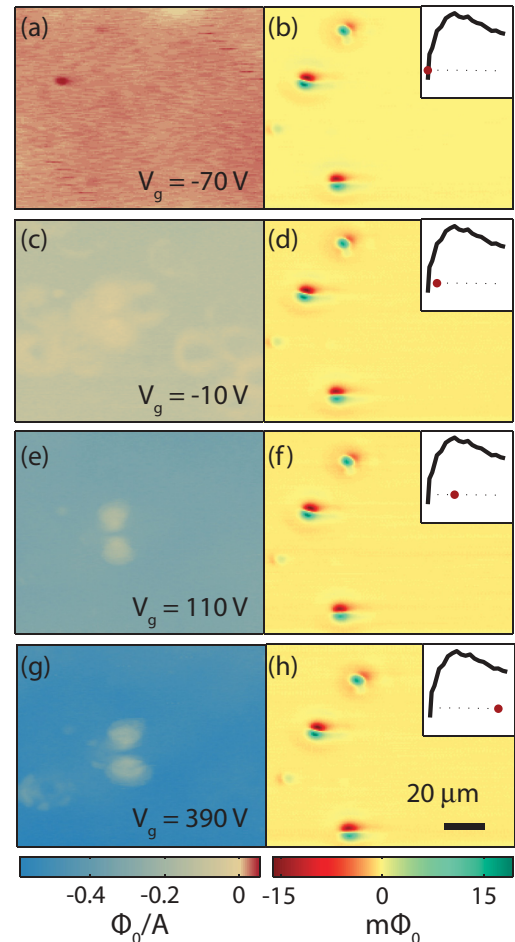


FIG. 4. (Color) Susceptometry (left) and magnetometry (right) at 80 mK at different gate voltages. Inset: Reproduction of the T_c dome from Fig. 1 showing the relative location of V_g in each panel. (a), (b) The sample is no longer superconducting and has a paramagnetic response. Individual ferromagnetic dipoles are also visible in the paramagnetic image. (c), (d) Superconductivity appears and the landscape is relatively inhomogeneous. (e), (f) Peak of the superconducting dome, most inhomogeneity disappears. (g), (h) Excess inhomogeneity returns on the overdoped side of the dome. The ring shapes in the inhomogeneous response match the dimensions of the SQUID's field coil and are likely due to disperse pointlike defects which interact strongly with the field coil. The ferromagnetic patches do not change with V_g and remain when superconductivity is gone.

change with V_g . The effect of RSOC on the band structure may depend on the chemical potential which is also tuned by the gate. Therefore the insensitivity of superconductivity to V_g cannot completely rule out a RSOC induced two-gap scenario. Yet, our second observation of the fast opening of the gap near T_c and the compatibility of the data with a single-gap BCS model limits two-gap models. Both gaps must be larger than the BCS s -wave gap to capture both the fast rise and flat low temperature dependence of the data.^{37,38}

Finally, disorder may play a role in washing out the triplet component. As stated above, the LAO/STO system is a dirty superconductor, with $\hbar/\tau \gg \Delta$. Disorder averaging has very little impact on the isotropic s -wave component but may eliminate the triplet component.

In short, our data is most consistent with a single gap. We cannot rule out the presence of two gaps, but our observations limit their size and V_g dependence.

Our scanning SQUID system allows two-dimensional mapping of superconductivity and magnetism at different V_g . Figure 4 shows simultaneously imaged susceptometry and magnetometry scans of the same region at 80 mK for four different V_g . The inhomogeneity in the diamagnetic screening is very large in the underdoped region ($V_g = -10$ V) and reenters the image in the overdoped region ($V_g = 390$ V). The least inhomogeneity is observed at optimal doping, although it does not disappear. In contrast, the ferromagnetic patches are insensitive to V_g with a constant magnitude and orientation for all V_g . This behavior was also observed on 15, 10, and 3.3 u.c. samples, showing the electron density that is modified by V_g does not appear to influence the ferromagnetism.

In conclusion, we presented measurements of the superfluid density as a function of temperature at multiple gate voltages throughout the superconducting dome in LAO/STO heterostructures. The temperature dependence of n_s is well described by a fully gapped BCS model. Moreover, the normalized n_s vs T curves collapse to a single functional form, indicating there is no change in the gap structure with V_g . Although we cannot rule out a two-gap mixed singlet/triplet model, the insensitivity of the superconducting state to V_g and the large slope near T_c limits two-gap scenarios. Specifically, both gaps must be larger than the BCS s -wave gap and their relative size cannot change throughout the dome. A future experiment to distinguish between these two scenarios may be to gate the superconductivity in the presence of an in-plane field, which can change the relative magnitude of triplet and singlet gaps. Alternatively, samples in the clean limit may reveal a clearer two-gap structure. Additionally, we found that the magnitude and orientation of the ferromagnetic patches that coexist with superconductivity are unchanged by V_g , while at the same time n_s goes from zero to 3.0×10^{12} cm⁻². This shows the population of electrons that is modified by the gate is separate from the electrons that contribute to the ferromagnetic order.

We thank S. A. Kivelson, E. A. Kim, M. H. Fischer, S. Raghu, A. Kampf, and I. Sochnikov for useful discussions and M. E. Huber for assistance in SQUID design and fabrication. Work was supported by the US Department of Energy, Office of Basic Energy Sciences, Materials Sciences and Engineering Division, under Award No. DE-AC02-76SF00515. B.K. acknowledges support from FENA. H.N. acknowledges support from a Stanford Graduate Fellowship. K.C.N. acknowledges support from NSF Grant No. DMR-0803974.

*kmoler@stanford.edu

¹C. H. Ahn, A. Bhattacharya, M. Di Ventra, J. N. Eckstein, C. D. Frisbie, M. E. Gershenson, A. M. Goldman, I. H. Inoue, J. Mannhart, A. J. Millis, A. F. Morpurgo, D. Natelson, and J. Triscone, *Rev. Mod. Phys.* **78**, 1185 (2006).

²A. Ohtomo and H. Y. Hwang, *Nature (London)* **427**, 423 (2004).

³D. G. Schlom and J. Mannhart, *Nat. Mater.* **10**, 168 (2011).

⁴N. Nakagawa, H. Y. Hwang, and D. A. Muller, *Nat. Mater.* **5**, 204 (2006).

⁵N. Reyren, S. Thiel, A. D. Caviglia, L. F. Kourkoutis, G. Hammerl, C. Richter, C. W. Schneider, T. Kopp, A. S. Rüetschi, D. Jaccard, M. Gabay, D. A. Muller, J. M. Triscone, and J. Mannhart, *Science* **317**, 1196 (2007).

⁶T. Sakudo and H. Unoki, *Phys. Rev. Lett.* **26**, 851 (1971).

⁷A. D. Caviglia, S. Gariglio, N. Reyren, D. Jaccard, T. Schneider, M. Gabay, S. Thiel, G. Hammerl, J. Mannhart, and J. M. Triscone, *Nature (London)* **456**, 624 (2008).

⁸C. Bell, S. Harashima, Y. Kozuka, M. Kim, B. G. Kim, Y. Hikita, and H. Y. Hwang, *Phys. Rev. Lett.* **103**, 226802 (2009).

⁹M. Ben Shalom, M. Sachs, D. Rakhmilevitch, A. Palevski, and Y. Dagan, *Phys. Rev. Lett.* **104**, 126802 (2010).

¹⁰A. Joshua, S. Pecker, J. Ruhman, E. Altman, and S. Ilani, *arXiv:1110.2184*.

¹¹A. D. Caviglia, M. Gabay, S. Gariglio, N. Reyren, C. Cancellieri, and J. M. Triscone, *Phys. Rev. Lett.* **104**, 126803 (2010).

¹²A. Fête, S. Gariglio, A. D. Caviglia, J. M. Triscone, and M. Gabay, *arXiv:1203.5239*.

¹³J. A. Bert, B. Kalisky, C. Bell, M. Kim, Y. Hikita, H. Y. Hwang, and K. A. Moler, *Nat. Phys.* **7**, 767 (2011).

¹⁴L. Li, C. Richter, J. Mannhart, and R. C. Ashoori, *Nat. Phys.* **7**, 762 (2011).

¹⁵D. A. Dikin, M. Mehta, C. W. Bark, C. M. Folkman, C. B. Eom, and V. Chandrasekhar, *Phys. Rev. Lett.* **107**, 056802 (2011).

¹⁶K. Michaeli, A. C. Potter, and P. A. Lee, *Phys. Rev. Lett.* **108**, 117003 (2012).

¹⁷F. Loder, A. Kampf, and T. Kopp, *arXiv:1206.1816*.

¹⁸B. Liu and X. Hu, *Phys. Rev. B* **81**, 144504 (2010).

¹⁹B. Kalisky, J. A. Bert, B. B. Klopfer, C. Bell, H. K. Sato, M. Hosoda, Y. Hikita, H. Y. Hwang, and K. A. Moler, *Nat. Commun.* **3**, 922 (2012).

²⁰P. G. Björnsson, B. W. Gardner, J. R. Kirtley, and K. A. Moler, *Rev. Sci. Instrum.* **72**, 4153 (2001).

²¹J. Pearl, *Appl. Phys. Lett.* **5**, 65 (1964).

²²V. G. Kogan, *Phys. Rev. B* **68**, 104511 (2003).

- ²³A. D. Caviglia, S. Gariglio, C. Cancellieri, B. Saccpe, A. Fete, N. Reyren, M. Gabay, A. F. Morpurgo, and J. M. Triscone, *Phys. Rev. Lett.* **105**, 236802 (2010).
- ²⁴See Supplemental Material at <http://link.aps.org/supplemental/10.1103/PhysRevB.86.060503> for a discussion of our systematic errors.
- ²⁵C. C. Homes, S. V. Dordevic, D. A. Bonn, R. Liang, and W. N. Hardy, *Phys. Rev. B* **69**, 024514 (2004).
- ²⁶Similar behavior was seen in a separate 10 u.c. sample.
- ²⁷See Supplemental Material at <http://link.aps.org/supplemental/10.1103/PhysRevB.86.060503> for the details of the phenomenological model.
- ²⁸R. Prozorov and R. W. Giannetta, *Supercond. Sci. Technol.* **19**, R41 (2006).
- ²⁹F. Gross, B. S. Chandrasekhar, D. Einzel, K. Andres, P. J. Hirschfeld, H. R. Ott, J. Beuers, Z. Fisk, and J. L. Smith, *Z. Phys. B* **64**, 175 (1986).
- ³⁰J. P. Carbotte, *Rev. Mod. Phys.* **62**, 1027 (1990).
- ³¹R. Prozorov and V. G. Kogan, *Rep. Prog. Phys.* **74**, 124505 (2011).
- ³²V. J. Emery and S. A. Kivelson, *Nature (London)* **374**, 434 (1995).
- ³³V. L. Pokrovskii, *JETP Lett.* **47**, 629 (1988).
- ³⁴C. S. Koonce, M. L. Cohen, J. F. Schooley, W. R. Hosler, and E. R. Pfeiffer, *Phys. Rev.* **163**, 380 (1967).
- ³⁵R. Winkler, *Spin-Orbit Coupling Effects in Two-Dimensional Electron and Hole Systems* (Springer, Berlin, 2003).
- ³⁶P. A. Frigeri, D. F. Agterberg, A. Koga, and M. Sgrist, *Phys. Rev. Lett.* **92**, 097001 (2004).
- ³⁷See Supplemental Material at <http://link.aps.org/supplemental/10.1103/PhysRevB.86.060503> for a discussion of multiple gaps.
- ³⁸L. Luan, T. M. Lippman, C. W. Hicks, J. A. Bert, O. M. Auslaender, J. Chu, J. G. Analytis, I. R. Fisher, and K. A. Moler, *Phys. Rev. Lett.* **106**, 067001 (2011).